

# Toward automatic estimation of urban green volume using airborne LiDAR data and high resolution Remote Sensing images

Yan HUANG<sup>1</sup>, Bailang YU (✉)<sup>1</sup>, Jianhua ZHOU<sup>1</sup>, Chunlin HU<sup>2</sup>, Wenqi TAN<sup>2</sup>, Zhiming HU<sup>1</sup>, Jianping WU<sup>1</sup>

<sup>1</sup> Key Laboratory of Geographic Information Science (Ministry of Education), East China Normal University, Shanghai 200241, China

<sup>2</sup> Shanghai Landscape and City Appearance Administration Information Center, Shanghai 200040, China

© Higher Education Press and Springer-Verlag Berlin Heidelberg 2012

**Abstract** Urban green volume is an important indicator for analyzing urban vegetation structure, ecological evaluation, and green-economic estimation. This paper proposes an object-based method for automated estimation of urban green volume combining three-dimensional (3D) information from airborne Light Detection and Ranging (LiDAR) data and vegetation information from high resolution remotely sensed images through a case study of the Lujiazui region, Shanghai, China. High resolution airborne near-infrared photographs are used for identifying the urban vegetation distribution. Airborne LiDAR data offer the possibility to extract individual trees and to measure the attributes of trees, such as tree height and crown diameter. In this study, individual trees and grassland are identified as the independent objects of urban vegetation, and the urban green volume is computed as the sum of two broad portions: individual trees volume and grassland volume. The method consists of following steps: generating and filtering the normalized digital surface model (nDSM), extracting the nDSM of urban vegetation based on the Normalized Difference Vegetation Index (NDVI), locating the local maxima points, segmenting the vegetation objects of individual tree crowns and grassland, and calculating the urban green volume of each vegetation object. The results show the quantity and distribution characteristics of urban green volume in the Lujiazui region, and provide valuable parameters for urban green planning and management. It is also concluded from this paper that the integrated application of LiDAR data and image data presents an effective way to estimate urban green volume.

**Keywords** urban green volume, LiDAR, remote sensing image, object-based method, automatic estimation

## 1 Introduction

As an important ecological component in urban ecosystem, urban vegetation plays an important role in improving the quality of the urban environment and maintaining urban ecological balance (Morancho, 2003; Tyrväinen et al., 2007). It can mitigate the urban heat island effect (Weng et al., 2004), reduce CO<sub>2</sub> emissions (Akbari, 2002), decrease street noise (Fang and Ling, 2003), and sequester the carbon in atmospheric air (Awal et al., 2010). At the same time, different types of vegetation, such as trees, shrubs, and grasses, have varying capacities for benefiting the urban environment. Therefore, with an optimized structure and rational layout, urban vegetation can maximize ecological benefits within a limited urban space. In this situation, an indicator representing the two-dimensional (2D) distribution as well as the three-dimensional (3D) vegetation structure should be selected when evaluating ecological benefits and environmental advantages of urban vegetation (Zhou, 2001; Zhu, 2008). Green volume, unlike timber volume/standing tree volume (the volume occupied by woody tissues) (Lefsky and McHale, 2008), is defined as the total volume of green plant stems and leaves above the ground (Zhou and Sun, 1995; Hecht et al., 2008). As an important indicator of vegetation, urban green volume quantitatively describes the vegetation space structure and the relationship between the vegetation and environment. Thus, the accurate and updated urban green volume of specific regions within a city is essentially important for urban ecosystems research, urban planning, and government decision-making.

Traditionally, green volume is estimated based on field

measurement. Height and crown diameter of individual trees are measured by line gauge and other instruments. An empirical formula is adopted to transfer the observed parameters to the estimated green volume (Zhou and Sun, 1995). It is often labor-expensive and time-consuming to acquire particular attributes (such as species, height, and crown diameter) of individual trees in a large area. In recent decades, various remote sensing (RS) techniques have been employed in investigating vegetation distribution and estimating green volume. Multi-spectral remotely sensed images can provide reliable spectral information, which is beneficial to derive the distribution and 2D structure of vegetation. For example, Chen and Gillieson (2009) estimated vegetation cover in semi-arid rangeland environments by using five Landsat Thematic Mapper spectral bands and 17 vegetation indices. However, the vertical parameter of urban vegetation cannot be acquired from RS photographs directly. Thus, the methods consist of derivation of 3D information (crown diameter and tree height) followed by empirical formulas computation are always employed to compute green volume based on optical RS images. For example, Zhou (2001) identified tree species from RS images manually, and then the relationships between crown diameter and crown height of each species were set by using regression analysis. Zhou et al. (2005) proposed a green-shade method for calculating tree height using the tree-shadow length derived from aerial RS images. Hall et al. (2006) modeled forest stand volume using empirical relationships between the estimates of forest structure attributes and the spectral response variables from Landsat ETM+ image. Ozdemir (2008) investigated the relationship between stem volume and tree attributes (tree crown area and tree shadow area) which are measured from pan-sharpened Quickbird imagery in a Crimean juniper forest. Although these studies derived the 3D parameters of vegetation, they suffer from the drawbacks of complicated procedures and poor accuracy of results.

As a technological breakthrough in obtaining 3D information of objects, an airborne Light Detection and Ranging (LiDAR) system provides a quick and cost-effective way to survey and map surface topography. Due to its dense sampling density and accurate measurements, LiDAR data can be used to represent the urban 3D morphology (Yu et al., 2009a; Yu et al., 2010) and to measure the vertical structure of individual trees (Hudak et al., 2002). It is also proven that airborne LiDAR data are effective in obtaining tree attributes (Magnussen et al., 1999; Means et al., 2000; Naesset and Okland, 2002; Persson et al., 2002; Vêga and Durrieu, 2011) and to estimate green volume (Nilsson, 1996; Naesset, 1997; Hecht et al., 2008; Dalponte et al., 2011). However, the exclusive utilization of LiDAR data is inadequate for identifying objects with similar 3D morphological properties (e.g., open space and lawn). For these reasons, the combination of 3D morphological information from

LiDAR data and spectral information from image data shows great promise. Several works related to green volume estimation combining LiDAR data with image data have already been reported in the literatures (Hyypä et al., 2000; Leckie et al., 2003; Takahashi et al., 2010; Tonolli et al., 2011). For example, tree stem volume is measured by using the high pulse rate laser scanner and aerial photography (Hyypä et al., 2000). And this method is suitable for inventory investigation at the stand level especially in the forests with homogeneous structure. Takahashi et al. (2010) estimated the stand volume in closed-canopy Japanese cedar plantations combining low-density LiDAR data with QuickBird panchromatic imagery by using an empirical model, which was constructed based on individual stem volume, tree height, and crown projection area. This method is suitable for offering precise stand volume estimates in coniferous forests in different localities. All the studies mentioned above offer potential for estimating green volume in urban areas.

Object-based methods, which target image objects rather than individual pixels as the basic unit, is regarded as a new approach for image analysis and understanding (Yu et al., 2009b; Blaschke and Strobl, 2001). The objects recognized by specific algorithms can correspond better to concerned components and provide extra information (e.g., semantic information of individual object and spatial relationships between objects) that individual pixels cannot offer (Blaschke, 2010). This paper presents a new integrated route to automatically estimate object-based urban green volume using airborne LiDAR data and high resolution images. In this study, individual trees and grassland are considered as the component objects of urban vegetation. The airborne LiDAR data are used for extracting individual trees and measuring the attributes of trees, such as stem location, tree height, and crown diameter. The high resolution near-infrared airborne remotely sensed photographs are utilized to identify the urban vegetation distribution. The rest of this paper will be organized as follows. A detailed description of study area and data will be first provided. Then the estimated methods will be introduced. This will be followed by the presentation of analytic results and their discussions. To close, we will draw conclusions.

---

## 2 Study area and data

### 2.1 Study area

The Lujiazui region, which is on the east bank of the Huangpu River, is the most famous financial and trade center in downtown Shanghai, China. Many prominent commercial and banking companies have set up their agencies in this region. Large numbers of various man-made objects, such as skyscrapers and residential build-

ings, cluster round in this area. The vegetation distribution in the region is composed of greenbelts in parks and residential areas, gardens in commercial districts, and street trees. Lujiazui represents one of the most multifarious urban landscapes crowded with structures of different natures and heights. In this paper, a rectangular portion of the Lujiazui region with an approximate area of 300 ha is selected as the case study area (Fig. 1).

## 2.2 Data

The high resolution (1 m spatial resolution) RS image used in this study was acquired in February, 2006 (Fig. 1). The image contains three spectral bands: green, red, and near-infrared.

The airborne LiDAR data collected by the Optech ALTM 3100 system on February, 2006 was provided by the Geomatics Center at Shanghai Municipal Institute of Surveying and Mapping (Feng et al., 2008). The LiDAR point measurements of the first return were provided as  $x$ ,  $y$ ,  $z$  lists in an ASCII file. According to the metadata, the mean accuracy of LiDAR measurements is estimated to be about 10 cm and the average sampling density is 1 point per 0.6 m<sup>2</sup>.

To provide the validation data set, the information of individual trees (trees along the roadsides and in the Shanghai Lujiazui Central Greenbelt), which recorded the species and stem location of each tree, was supplied by the Shanghai Municipal Administration of Urban Afforesting and Appearance. The species and stem location of individual trees were collected from in situ measurements in 2006 and updated annually.

## 3 Methods

The objective of our method is to derive different types of vegetation objects, including objects of individual trees and grasslands, automatically. Each object will be assigned a specific equation for green volume estimation. The parameter value of the equation for a specific object is defined from its own attributes. The objects of individual trees and grasslands are segmented layer by layer. The definition of operational targets in each layer and the description of their properties are the basis of our method. As shown in the hierarchical structure and essential attributes of vegetation objects (Fig. 2), it involves three layers of targets. The original layer is the whole study area, which contains both height information from normalized digital surface model (nDSM) and spectral attributes from RS images. Based on the spectral information of RS images, the study area is divided into two portions—vegetation surface and non-vegetation surface. Moreover, vegetation surface not only inherits the initial height value, but also possesses a new category attribute—“vegetation.” In view of the inhomogeneity in the internal structure, the vegetation surface is subdivided into two classes of objects: objects of individual trees and objects of grassland according to the height value and the relationship with neighborhood. Consequently, the vegetation objects used in urban volume estimation refer to the objects in third layer (i.e., objects of grassland and individual trees). Each vegetation object has the particular attributes: height, area, and corresponding equation for green volume calculation.

The method we propose to estimate urban green volume targets vegetation objects as the analysis units, and the



Fig. 1 Geographic location and airborne near-infrared images of the Lujiazui region, Shanghai, 2006

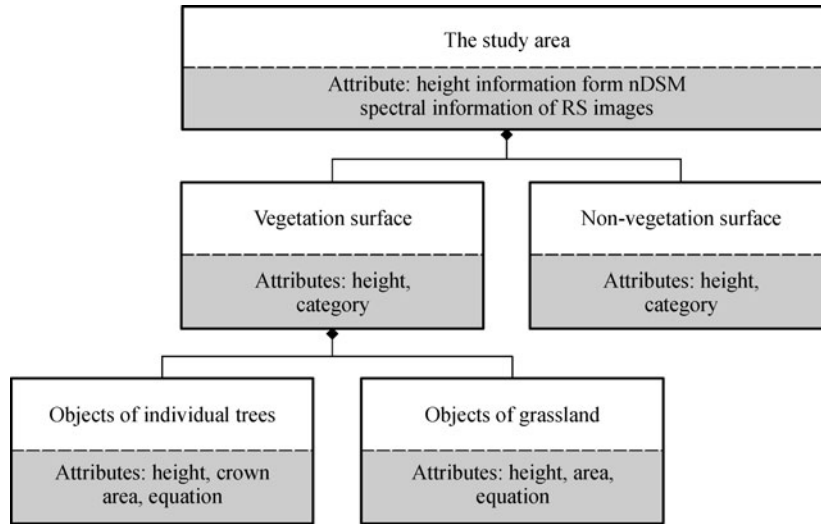


Fig. 2 The hierarchical structure and essential attributes of vegetation objects

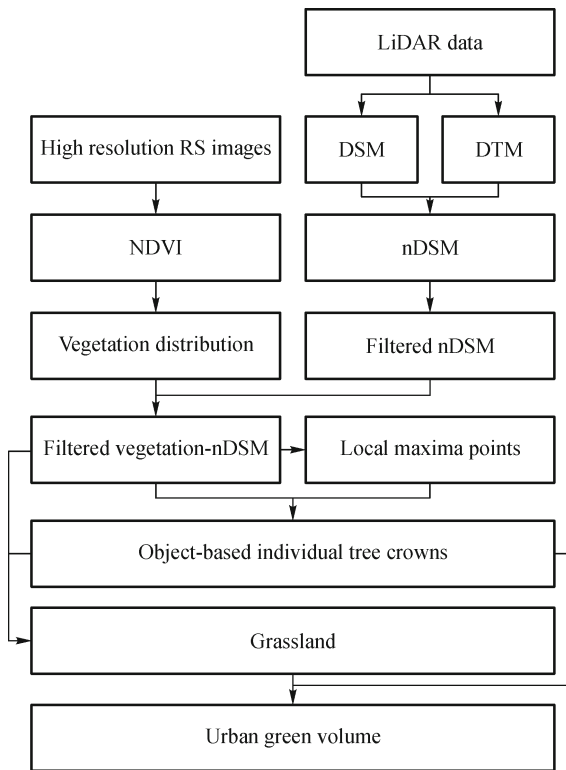


Fig. 3 The procedure of urban green volume estimation

process routing includes following five steps (Fig. 3): (i) generating and filtering nDSM, (ii) extracting the vegetation-covered part of nDSM (Vegetation-nDSM), (iii) locating the local maximum points, (iv) segmenting the objects of individual tree crowns and grassland, and (v) calculating the urban green volume.

### 3.1 Generating and filtering nDSM

The nDSM is the difference between the digital surface model (DSM) and the digital terrain model (DTM). First, ground points are extracted by removing non-ground measurements from the original airborne LiDAR point cloud by using a progressive morphological filter (Zhang et al., 2003) provided in the Airborne LiDAR Data Processing and Analysis Tools 1.0 (ALDPAT 1.0, see <http://lidar.ihr.fiu.edu/lidartool.html>). Then, a TIN layer is created from the original LiDAR points, and a DSM grid with 1 m cell size (same as the resolution of RS image) is interpolated by linear interpolation from the TIN layer. These processes have been proven by Yu et al. (2009a, 2010) to decrease interpolation error. Next, a DTM grid with 1 m cell size is also interpolated from the ground points. Finally, the nDSM (Fig. 4) of the Lujiazui region is generated by subtracting the DTM from the DSM (Eq. (1)). The TIN creation, DSM interpolation, and nDSM generation are accomplished with ArcGIS 9.3 software.

$$nDSM = DSM - DTM. \quad (1)$$

To reduce the noise and emphasize the identification of individual trees, the original nDSM is filtered with a Gaussian low-pass  $3 \times 3$  filter (Eq. (2)) (Hyypä et al., 2001). The example area shown in Fig. 4 is used in Fig. 5 to illustrate the processes of our method. Figure 5(b) is the original nDSM. The result of filter is shown in Fig. 5(c). After that, the height attributes of the whole study area is set by using the smoothed nDSM.

$$\begin{bmatrix} 1 & 2 & 1 \\ 2 & 4 & 2 \\ 1 & 2 & 1 \end{bmatrix} / 16. \quad (2)$$

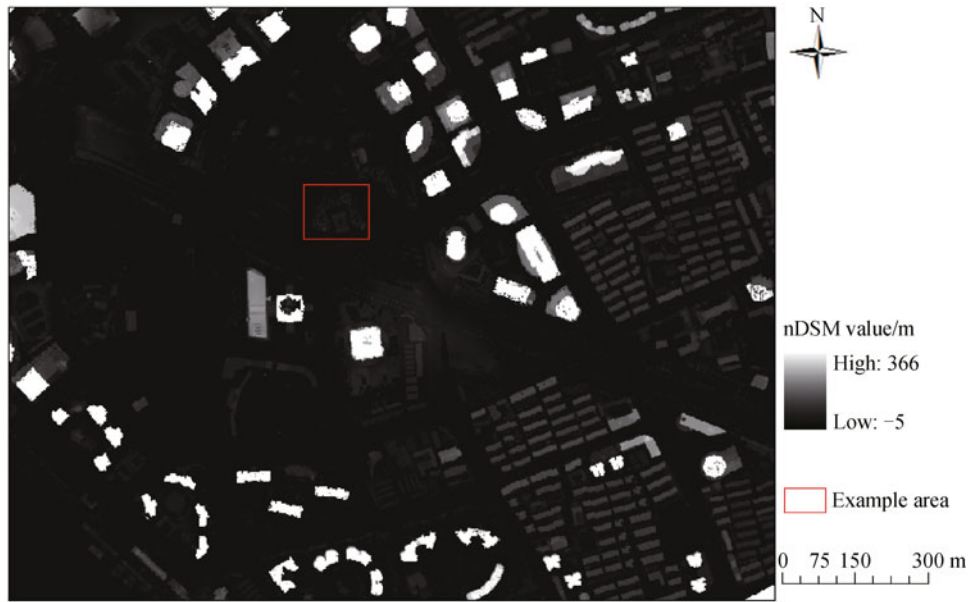


Fig. 4 The nDSM of the Lujiazui region from airborne LiDAR data (2006)

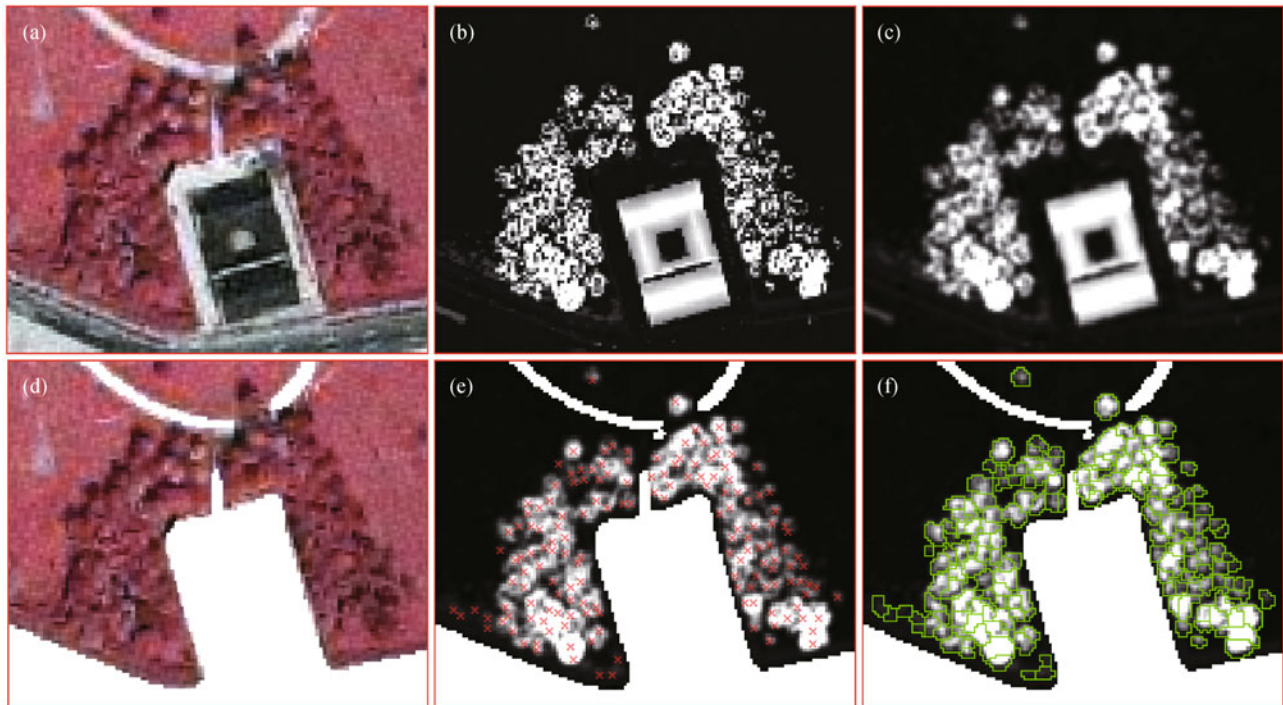


Fig. 5 Illustration of identifying individual tree objects by using airborne LiDAR data and near-infrared RS images. (a) Original high resolution airborne near-infrared photograph; (b) original nDSM; (c) filtered nDSM; (d) high resolution airborne near-infrared photograph after extracting vegetation; (e) local maximum points (red crosses) based on filtered nDSM of urban vegetation; (f) segmented results of individual tree crown objects (green pseudo-circles)

### 3.2 Extracting vegetation-nDSM

As mentioned before, objects with similar 3D morphological characteristics cannot be classified by using airborne LiDAR data alone. The spectral information from

near-infrared RS images is adapted to derive the vegetation distribution. To emphasize the vegetation factor, the Normalized Difference Vegetation Index (NDVI) is calculated based on the near-infrared band and red band of the image. To facilitate the automatic process in the

method, a threshold-value-based method is used to extract the vegetation surface. In our method, the pixels whose NDVI values are larger than 0 are defined as the vegetation surface (Fig. 5(d)). After masking the filtered nDSM with the vegetation surface, the filtered vegetation-nDSM of the Lujiazui region (Fig. 5(e)) is extracted.

### 3.3 Locating the local maximum points

This step is based on the height value in the masked nDSM. If a pixel has the highest value compared with all of its eight neighbors, the pixel is defined as a local maximum point, namely the top of a tree (Hyypä et al., 2001). To extract the trees from urban vegetation, only points whose height range from 1 to 30 m are considered in this study (Fig. 5(e)). The 1 m is for removing the grassland and the 30 m is for removing artificial vegetation on the top of buildings.

### 3.4 Segmenting the objects of individual tree crowns and grassland

The vegetation surface of the Lujiazui region is successfully extracted using NDVI. Then the detailed method to segment vegetation objects based on the height information are introduced. The objects of individual tree crowns, which usually manifest the individual trees in two-dimensional images, are modeled from each local maximum point based on the neighbor algorithm (Véga and Durrieu, 2011). First, each maximum point is regarded as a seed point and marked with a unique label (1, 2, 3, ...,  $k$ ). Next, the neighborhood search will start from the seed point labeled with 1. If there is no eligible neighbor in the eight directions, the search will move to the next seed point. For each tested nDSM pixel in eight neighbors, if its value and two of its neighbors' value are lower than the center pixel, this pixel is thought to be a part of the crown. In addition, for controlling the outer boundary of the tree crown, the tested neighbor's value should be above a threshold. In this study, multiple threshold values are set based on the height of seed points. A threshold of 0.6 m is set for those tree seed points which height values are from 1 to 2 m, 0.8 m is for the values from 2 to 5 m, and 1.2 m is for the rest. Only when all of the conditions mentioned above are met will the tested neighbor pixel be added to the tree crown and marked with the same label as the original tree seed point. Then, the search will resume based on the pixels which were just added in the last step. The neighborhood search ends when there is no candidate pixel located in the crown pixels' eight neighbor. After the search, only the trees which have a crown pixel number greater than 0 are retained.

After recognizing the individual tree crowns, each tree object possesses the essential attributes (such as tree height and crown area), which are the crucial indices for accuracy assessment and green volume estimation. The quality of

segmented individual tree crowns is assessed by using 104 sample trees. Since the absence of measured information about the tree height, crown diameter as the same period as RS image (February, 2006), a visual interpretation was adopted instead. A sample region appropriate for identifying the location and profile of individual trees is selected from the filtered nDSM. Then, the segmented tree crown area is compared with the interpretation result (Fig. 6). The root-mean-square error (RMSE) is 1.66 m.

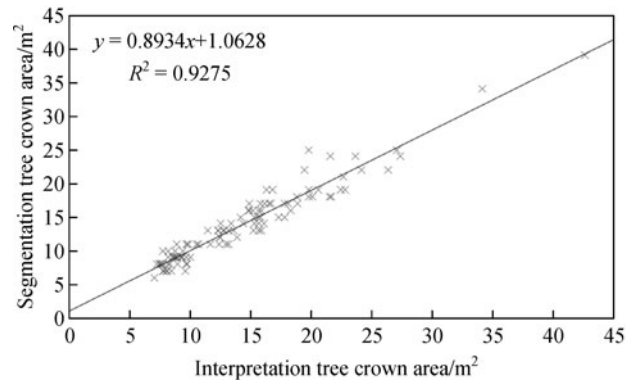


**Fig. 6** Segmented tree crown area compared with interpreted tree crown area

The objects of grassland are extracted by removing the individual trees from the vegetation surface. Due to the homogeneity of space structure, the height of all the grassland objects are assumed the same. In this paper, 0.12 m identifies the height of all grassland objects (generally, the height of grassland in urban areas is 0.10–0.12 m).

### 3.5 Calculating the urban green volume

The urban green volume is the sum volume of individual tree objects and grassland objects. For the volume estimation of individual tree objects, the segmented tree crown and corresponding tree height are first used to generate a series of pseudo-cylinders. These pseudo-cylinders reveal the morphological characteristics of individual trees in the form of optimum-fitting cylinder. For each pseudo-cylinder, the diameter of underside pseudo-circle defines crown diameter, and the height defines tree height. Then, those pseudo-cylinders are further reconstructed into individual tree objects as a result of comprehensive consideration of crown diameter and tree height. To each object is added a new attribute: volume equation (Eq. (3)). The morphological parameter ( $K$ ) is defined in Eq. (4).

$$V_T = S_T \times H_T \times K, \quad (3)$$

where  $V_T$  is the volume of individual tree object,  $S_T$  is the crown area of tree object,  $H_T$  is the height of tree object, and  $K$  is the morphological parameter between pseudo-cylinder and individual tree objects.

$$K = \begin{cases} 0.7 (D_{\text{Crown}} \geq 10 \text{ m and } 1 \text{ m} \leq H_{\text{Tree}} < 10 \text{ m}) \\ 0.6 (D_{\text{Crown}} \geq 10 \text{ m and } H_{\text{Tree}} \geq 10 \text{ m}) \\ 0.5 (5 \text{ m} \leq D_{\text{Crown}} < 10 \text{ m and } 5 \text{ m} \leq H_{\text{Tree}} < 10 \text{ m}) \\ \text{or } (1 \text{ m} \leq D_{\text{Crown}} < 5 \text{ m and } 1 \text{ m} \leq H_{\text{Tree}} < 5 \text{ m}) \\ 0.35 (5 \text{ m} \leq D_{\text{Crown}} < 10 \text{ m and } H_{\text{Tree}} \geq 10 \text{ m}) \\ 0.45 (\text{otherwise}) \end{cases}, \quad (4)$$

where  $D_{\text{Crown}}$  is the diameter of tree crown,  $H_{\text{Tree}}$  is the height of tree.

The volume equation of grassland objects is depicted in Eq. (5):

$$V_G = S_G \times H_G, \quad (5)$$

where  $V_G$  is the volume of grassland object,  $S_G$  is the area of grassland object, and  $H_G$  is 0.12 m.

## 4 Implementation and software tools

The automatic estimation of urban green volume proposed in this paper has been implemented as an ArcGIS 9.3 extension module with a graphical user interface (GUI). The GUI is designed by employing Microsoft Visual Studio 2008 platform, and the algorithms are coded by using the C# programming language.

This extension model is a generic software tool (Fig. 7)

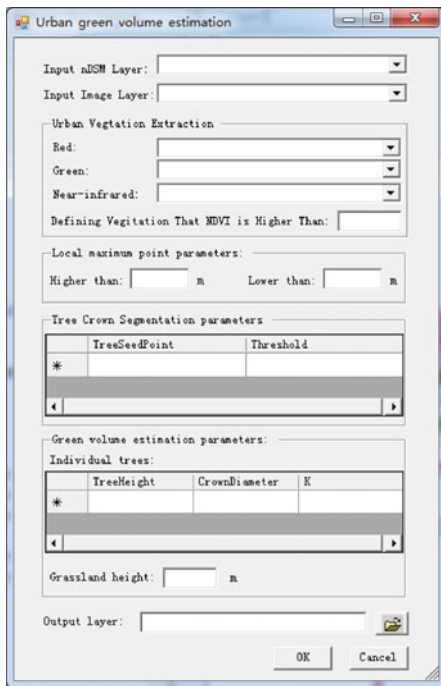


Fig. 7 The software tool for automatic estimation of urban green volume

to automatically estimate urban green volume. The input data includes the LiDAR, nDSM, and the RS image. In addition, a series of parameters used for urban vegetation extraction, local maximum point parameters, tree crown segmentation parameters, and urban green volume estimation are required user input. First, the red, green, and near-infrared bands must be selected in accordance with the input RS data, and the NDVI threshold for extracting the urban vegetation object defined. Secondly, the height range of retained local maximum points must be appointed. Thirdly, users must set the threshold on the basis of tree seed point (local maximum point) for segmenting individual tree crowns. Finally, the morphological parameter  $K$  (depending on tree height and tree crown diameter) of individual tree objects and the height of grassland object must be defined. The output is a vector data layer of vegetation objects, which recorded the object category (individual tree or grassland), height, area, and green volume. During the operation, users can customize the related parameters in each step, and the estimation result also can be associated with other GIS data for further urban ecological environment assessment and management.

## 5 Results and discussion

### 5.1 Segmentation of individual tree objects and grassland objects

The segmentation result of vegetation objects is shown in a 3D-view (Fig. 8). The total crown area of individual tree objects is 110218 m<sup>2</sup>, corresponding to 22.27% of the vegetation objects. And the area of grassland objects is 384677 m<sup>2</sup>, corresponding to 77.73%. Compared with the RS image, we find that the sizes of tree objects, especially those along the sides of roads, are underestimated. The minimum tree height is only 1.05 m. According to the reference information of tree species, these underestimated tree objects along the roads are mainly *Platanus acerifolia* (Ait.) Willd and *Cinnamomum camphora* (L.) Presl. The *P. acerifolia* (Ait.) Willd is a typical deciduous tree, which is still bare in February. In addition, as LiDAR tends to miss absolute treetops, which has been pointed out in other results (Popescu et al., 2002; Popescu, 2007), the tree height and tree crown diameter may be lower than the actual value.

### 5.2 Estimated green volume and accuracy assessment

The green volume of individual tree objects are evaluated with the results, which are calculated using the green equation proposed by Zhou and Sun (1995) (Fig. 9). For the green equation, different species of trees have different tree crown geometries, hence the green volume of each tree



**Fig. 8** The 3D-view of vegetation objects

**Table 1** The parameters and green equations of individual tree object

Tree species	The correlation equation of crown diameter and crown height: * $y = 1/(a + b e^{-cx})$			The volume equation of individual tree object*
	<i>a</i>	<i>b</i>	<i>c</i>	
<i>Cinnamomum camphora</i> (L.) Presl	0.086886	2.886574	0.57	$\pi x^2 y/6$
<i>Ginkgo biloba</i> L.	0.027305	0.170260	0.09	$\pi x^2 y/12$
<i>Magnolia grandiflora</i> Linn.	0.047223	0.941057	0.37	$\pi x^2 y/6$
<i>Magnolia denudata</i> Desr.	0.122672	1.052523	0.67	$\pi x^2 y/6$
<i>Cedrus deodara</i> (Roxb.) G. Don	0.080197	0.743925	0.47	$\pi x^2 y/12$
<i>Metasequoia glyptostroboides</i> Hu et Cheng	0.038946	1.206990	0.77	$\pi x^2 y/12$
<i>Sabina chinensis</i> cv. Kaizuka	0.069298	5.265099	1.27	$\pi x^2 y/12$
<i>Salix babylonica</i> L.	0.095657	365.5584	2.27	$\pi x^2 y/6$
<i>Platanus acerifolia</i> (Ait.) Willd	0.105595	1.534633	0.39	$\pi x^2 y/6$

Note: \* *x* is the crown diameter, *y* is the crown height

species is estimated according to its specific equation. Along with the species information from in situ measurements, the objects of individual trees are mainly classified into nine species (*Cinnamomum camphora* (L.) Presl, *Ginkgo biloba* L., *Magnolia grandiflora* Linn., *Magnolia denudata* Desr., *Cedrus deodara* (Roxb.) G. Don, *Metasequoia glyptostroboides* Hu et Cheng, *Sabina chinensis* cv. Kaizuka, *Salix babylonica* L., and *Platanus acerifolia* (Ait.) Willd). First, the crown height is acquired using the correlation equation of crown diameter and crown height, and then the volume of each individual tree object is calculated through the crown diameter and crown height. The specific equations for each species are in Table 1. The total amount of green volume estimated by Eq. (3) is 63216.96 m<sup>3</sup>, which corresponds to 66361.29 m<sup>3</sup> using Zhou's equation (Zhou and Sun, 1995). The relative accuracy is 95.26%.

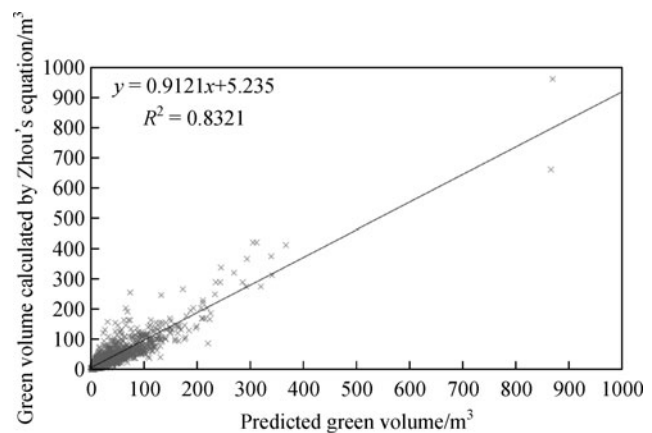


**Fig. 9** Estimated green volume compared with the green volume calculated by Zhou's equation



Our results show that the total green volume of the Lujiazui region is  $353317.66 \text{ m}^3$ . To further analyze the distribution characteristics of green volume in the region, the mean green volume based on block and grids ( $10 \text{ m} \times 10 \text{ m}$ ) in Lujiazui is calculated. Figure 10 shows the distribution of block-based mean green volume. We find that the mean green volume of parks and north-east residence communities is highest ( $0.30\text{--}0.61 \text{ m}^3/\text{m}^2$ ), followed by Century Ave. and Century Ave. to the south of residence communities ( $0.20\text{--}0.30 \text{ m}^3/\text{m}^2$ ), high-rise commercial office areas ( $0.20\text{--}0.30 \text{ m}^3/\text{m}^2$ ), and most roads and under construction lands ( $0.10\text{--}0.20 \text{ m}^3/\text{m}^2$ ). The mean green volume of Pucheng Rd. and a small region located in the south-east is  $0 \text{ m}^3/\text{m}^2$ . This indicates that the parks and residential greenbelts are the main source of urban green volume, and the street trees and the commercial greenbelts need to be optimized in the future.

Combining the distribution of vegetation objects (Fig. 8) with the grids (Fig. 11), we can see that the mean green volume of grassland objects is  $0\text{--}0.50 \text{ m}^3/\text{m}^2$ , and the mean green volume of individual tree objects ranges from  $0.5$  to  $8.37 \text{ m}^3/\text{m}^2$ . This reveals that in the same coverage area, the green volume of individual tree objects is significantly higher than that of grassland objects. Therefore, to further increase the urban green volume, the green space structure should be optimized.

## 6 Conclusions

In this paper, an object-based method for automated estimation of green volume combining airborne LiDAR data with high resolution RS images has been proposed. It is demonstrated to be a useful and effective way to obtain urban green volume through a case study of the Lujiazui region, Shanghai, China. The implemented software module based on our method should be able to provide a powerful tool for the urban vegetation management department to rapidly monitor and measure the urban green volume.

In addition, the distribution pattern of urban green volume in the Lujiazui region can be summarized: in 2D, the parks and residential greenbelts are the main source of urban green volume, then the street trees and the commercial greenbelts. In 3D, the green volume per unit area of individual trees is significantly higher than that of grasslands, which indicates that the vegetation space structure has a great effect on environmental benefits of urban vegetation.

There are some underestimations (mainly for some individual trees along the roads) revealed from the results. The reason is the insufficient information that LiDAR data provided during leaf-off periods and the missing absolute treetops, which lead to the tree height and tree crown



**Fig. 10** The mean green volume in street blocks of the Lujiazui region

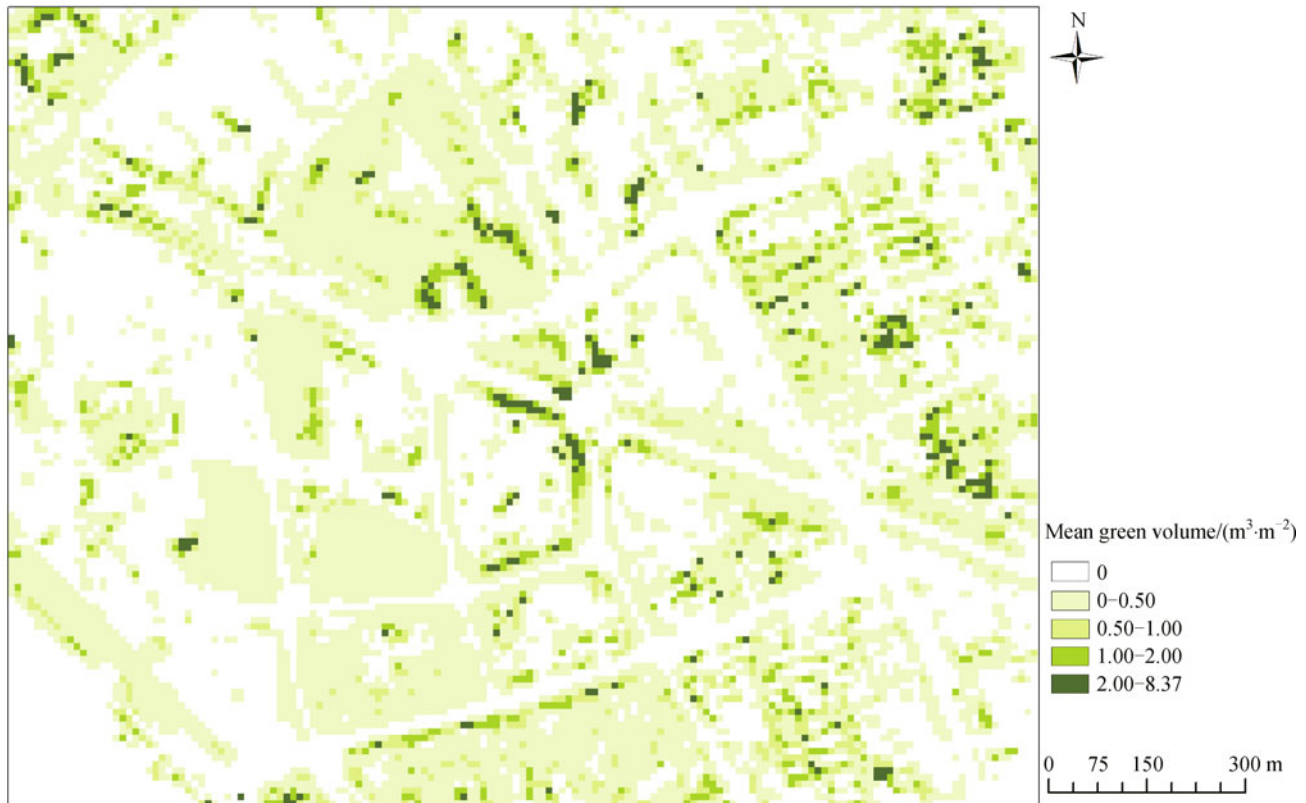


**Fig. 11** The mean green volume in grids (10 m × 10 m) of the Lujiazui region

diameter observations being lower than the real value. Because the tree crowns were defined as pseudo-circles, the segmentation morphology of tree crowns will be improved in a further study.

**Acknowledgements** This work is supported by the National Natural Science Foundation of China (Grant Nos. 41001270 and 41071275), the Specialized Research Fund for the Doctoral Program of Higher Education (Grant No. 20100076120017), and the Fundamental Research Funds for the Central Universities of China. We thank Prof. Ronghuan Guo and Dr. Yan Feng from Shanghai Municipal Institute of Surveying & Mapping to provide the LiDAR data.

## References

- Akbari H (2002). Shade trees reduce building energy use and CO<sub>2</sub> emissions from power plants. *Environ Pollut*, 116(Suppl 1): S119–S126
- Awal M A, Ohta T, Matsumoto K, Toba T, Daikoku K, Hattori S, Hiyama T, Park H (2010). Comparing the carbon sequestration capacity of temperate deciduous forests between urban and rural landscapes in central Japan. *Urban For Urban Green*, 9(3): 261–270
- Blaschke T (2010). Object based image analysis for remote sensing. *ISPRS J Photogramm Remote Sens*, 65(1): 2–16
- Blaschke T, Strobl J (2001). What's wrong with pixels? Some recent developments interfacing remote sensing and GIS. *Zeitschrift für Geoinformationssysteme*, 6(1): 12–17
- Chen Y, Gillieson D (2009). Evaluation of Landsat TM vegetation indices for estimating vegetation cover on semi-arid rangelands: a case study from Australia. *Can J Rem Sens*, 35(5): 435–446
- Dalponte M, Bruzzone L, Gianelle D (2011). A system for the estimation of single-tree stem diameter and volume using multireturn LIDAR data. *IEEE Trans Geosci Rem Sens*, 49(7): 2479–2490
- Fang C F, Ling D L (2003). Investigation of the noise reduction provided by tree belts. *Landsc Urban Plan*, 63(4): 187–195
- Feng Y, Guo R, Cheng Y (2008). Research on three dimensional city model reconstruction based on LiDAR. *Geomatics & Spatial Information Technology*, 31(4): 8–11 (in Chinese)
- Hall R J, Skakun R S, Arsenault E J, Case B S (2006). Modeling forest stand structure attributes using Landsat ETM+ data: application to mapping of aboveground biomass and stand volume. *For Ecol Manage*, 225(1–3): 378–390
- Hecht R, Meinel G, Buchroithner M F (2008). Estimation of urban green volume based on single-pulse LiDAR data. *IEEE Trans Geosci Rem Sens*, 46(11): 3832–3840
- Hudak A T, Lefsky M A, Cohen W B, Berterretche M (2002). Integration of lidar and Landsat ETM plus data for estimating and mapping forest canopy height. *Remote Sens Environ*, 82(2–3): 397–416
- Hyyppä J, Hyyppä H, Inkinen M, Schardt M, Ziegler M (2000). Forest inventory based on laser scanning and aerial photography. In: *Proceedings of SPIE, Laser Radar Technology and Applications V*, 4035: 106–573
- Hyyppä J, Kelle O, Lehtikoinen M, Inkinen M (2001). A segmentation-

- based method to retrieve stem volume estimates from 3-D tree height models produced by laser scanners. *IEEE Trans Geosci Rem Sens*, 39(5): 969–975
- Leckie D, Gougeon F, Hill D, Quinn R, Armstrong L, Shreenan R (2003). Combined high-density lidar and multispectral imagery for individual tree crown analysis. *Can J Rem Sens*, 29(5): 633–649
- Lefsky M, McHale M (2008). Volume estimates of trees with complex architecture from terrestrial laser scanning. *J Appl Remote Sens*, 2(1): 023521
- Magnussen S, Eggermont P, LaRiccia V N (1999). Recovering tree heights from airborne laser scanner data. *For Sci*, 45(3): 407–422
- Means J E, Acker S A, Fitt B J, Renslow M, Emerson L, Hendrix C J (2000). Predicting forest stand characteristics with airborne scanning lidar. *Photogramm Eng Remote Sensing*, 66(11): 1367–1371
- Moranco A B (2003). A hedonic valuation of urban green areas. *Landsc Urban Plan*, 66(1): 35–41
- Naesset E (1997). Estimating timber volume of forest stands using airborne laser scanner data. *Remote Sens Environ*, 61(2): 246–253
- Naesset E, Okland T (2002). Estimating tree height and tree crown properties using airborne scanning laser in a boreal nature reserve. *Remote Sens Environ*, 79(1): 105–115
- Nilsson M (1996). Estimation of tree heights and stand volume using an airborne LiDAR system. *Remote Sens Environ*, 56(1): 1–7
- Ozdemir I (2008). Estimating stem volume by tree crown area and tree shadow area extracted from pan-sharpened Quickbird imagery in open Crimean juniper forests. *Int J Remote Sens*, 29(19): 5643–5655
- Persson A, Holmgren J, Soderman U (2002). Detecting and measuring individual trees using an airborne laser scanner. *Photogramm Eng Remote Sensing*, 68(9): 925–932
- Popescu S C (2007). Estimating biomass of individual pine trees using airborne lidar. *Biomass Bioenergy*, 31(9): 646–655
- Popescu S C, Wynne R H, Nelson R F (2002). Estimating plot-level tree heights with lidar: local filtering with a canopy-height based variable window size. *Comput Electron Agric*, 37(1–3): 71–95
- Takahashi T, Awaya Y, Hirata Y, Furuya N, Sakai T, Sakai A (2010). Stand volume estimation by combining low laser-sampling density LiDAR data with QuickBird panchromatic imagery in closed-canopy Japanese cedar (*Cryptomeria japonica*) plantations. *Int J Remote Sens*, 31(5): 1281–1301
- Tonolli S, Dalponte M, Neteler M, Rodeghiero M, Vescovo L, Gianelle D (2011). Fusion of airborne LiDAR and satellite multispectral data for the estimation of timber volume in the Southern Alps. *Remote Sens Environ*, 115(10): 2486–2498
- Tyrväinen L, Makinen K, Schipperijn J (2007). Tools for mapping social values of urban woodlands and other green areas. *Landsc Urban Plan*, 79(1): 5–19
- Véga C, Durrieu S (2011). Multi-level filtering segmentation to measure individual tree parameters based on Lidar data: application to a mountainous forest with heterogeneous stands. *Int J Appl Earth Obs Geoinf*, 13(4): 646–656
- Weng Q, Lu D, Schubring J (2004). Estimation of land surface temperature-vegetation abundance relationship for urban heat island studies. *Remote Sens Environ*, 89(4): 467–483
- Yu B L, Liu H X, Wu J P, Hu Y J, Zhang L (2010). Automated derivation of urban building density information using airborne LiDAR data and object-based method. *Landsc Urban Plan*, 98(3–4): 210–219
- Yu B L, Liu H X, Wu J P, Lin W M (2009a). Investigating impacts of urban morphology on spatio-temporal variations of solar radiation with airborne LIDAR data and a solar flux model: a case study of downtown Houston. *Int J Remote Sens*, 30(17): 4359–4385
- Yu B L, Liu H X, Zhang L, Wu J P (2009b). An object-based two-stage method for a detailed classification of urban landscape components by integrating airborne LiDAR and color infrared image data: a case study of downtown Houston. In: *Proceedings of IEEE 2009 Joint Urban Remote Sensing Event*, Shanghai
- Zhang K, Chen S, Whitman D, Shyu M, Yan J, Zhang C (2003). A progressive morphological filter for removing nonground measurements from airborne LIDAR data. *IEEE Trans Geosci Rem Sens*, 41(4): 872–882
- Zhou J H (2001). Theory and practice on database of three-dimensional vegetation quantity. *Acta Geogr Sin*, 56(1): 14–23 (in Chinese)
- Zhou J H, Sun T Z (1995). Study on remote sensing model of three-dimensional green biomass and the estimation of environmental benefits of greenery. *Remote Sensing of Environment China*, 10(3): 162–174 (in Chinese)
- Zhou T G, Luo H, Guo D (2005). Remote sensing image-based quantitative study on urban spatial 3D green quantity virescence three-dimension quantity. *Acta Ecol Sin*, 25(3): 415–420 (in Chinese)
- Zhu J (2008). The value of green space vegetation quantity in afforestation planning and design. *Chinese Agricultural Science Bulletin*, 24(8): 360–363 (in Chinese)

## AUTHOR BIOGRAPHIES

**Yan Huang** received the B. S. degree in Geographical Information System from Chengdu University of Technology, Chengdu, China, in 2010. She is currently a Ph.D. student in Cartography and Geographical Information System at Department of Geography, East China Normal University, Shanghai, China. Her current research interests focus on object-oriented analysis for remotely sensed images and LiDAR. E-mail: hyansea@hotmail.com

**Bailang Yu** received the B. S. degree and Ph.D. degree from East China Normal University, Shanghai, China in 2002 and 2009, respectively. He is currently an Associate Professor of Key Laboratory of Geographic Information Science (Ministry of Education) and Department of Geography, East China Normal University. His research interests include object-oriented analysis for remotely sensed images, LiDAR, Urban Remote Sensing, and GIS (Geographical Information System). His recent research projects have been funded by the National Natural Science Foundation of China, the Specialized Research Fund for the Doctoral Program of Higher Education, and the Fundamental Research Funds for the Central Universities of China. E-mail: blyu@geo.ecnu.edu.cn

**Jianhua Zhou** received the B. E. degree in Aerial Photogrammetry from Wuhan Institute of Surveying and Mapping, Wuhan, China in 1975 and the M. S. degree in Cartography and Geographical Information System from East China Normal University, Shanghai, China in 2000. She is currently an Associate Professor of Key

Laboratory of Geographic Information Science (Ministry of Education) and Department of Geography, East China Normal University. Her research interests include quantitatively ecological remote sensing, remote sensing image analysis, and spatial data mining. E-mail: jhzhou@geo.ecnu.edu.cn

**Chunlin Hu** received the M. S. degree in Cartography and Geographical Information System from East China Normal University, Shanghai, China in 2004. She is currently an Engineer of Shanghai Landscape and City Appearance Administration Information Center. E-mail: hcl@lhsr.gov.cn

**Wenqi Tan** received the M. S. degree in Cartography and Geographical Information System from East China Normal University, Shanghai, China in 2005. She is currently an Engineer of Shanghai Landscape and City Appearance Administration Infor-

mation Center. E-mail: twq@lhsr.gov.cn

**Zhiming Hu** received the M. S. degrees in Cartography and Geographical Information System from East China Normal University, Shanghai, China in 2012. His research interests include mobile GIS and LiDAR. E-mail: zmhu031831@126.com

**Jianping Wu** received the B. S. degree from Nanjing University, Nanjing, China in 1983, the M. S. degree from Peking University, Beijing, China, in 1986, and the Ph.D. degree from East China Normal University, Shanghai, China, in 1996. He is currently a Professor of Key Laboratory of Geographic Information Science (Ministry of Education) and Department of Geography, East China Normal University, China. His research interests include Geographical Information System Development and Remote Sensing Application. E-mail: jpwu@geo.ecnu.edu.cn